Density-dependent electrical conductivity in suspended graphene: Approaching the Dirac point in transport

S. Das Sarma[1] and E. H. Hwang[1,2]

[1]*Condensed Matter Theory Center, Department of Physics, University of Maryland, College Park, Maryland 20742-4111, USA*

[2]*SKKU Advanced Institute of Nanotechnology, Sungkyunkwan University, Suwon 440-746, Korea*

(Received 15 November 2012; published 18 January 2013)

We theoretically consider, comparing with the existing experimental literature, the electrical conductivity of gated monolayer graphene as a function of carrier density, temperature, and disorder in order to assess the prospects of accessing the Dirac point using transport studies in high-quality suspended graphene. We show that the temperature dependence of graphene conductivity around the charge neutrality point provides information about how closely the system can approach the Dirac point, although competition between long-range and short-range disorder as well as between diffusive and ballistic transport may considerably complicate the picture. We also find that the acoustic phonon scattering contribution to the graphene resistivity is always relevant at the Dirac point, in contrast to higher density situations where the acoustic phonon contribution to the resistivity is strongly suppressed under the low-temperature Bloch-Grüneisen regime. We provide detailed numerical results for temperature- and density-dependent conductivity for suspended graphene.

DOI: 10.1103/PhysRevB.87.035415 PACS number(s): 72.80.Vp, 72.10.−d, 73.23.Ad

I. INTRODUCTION

It has been shown[1–6] that suspended graphene (SG) can achieve very high mobilities since various annealing techniques can remove much of the extrinsic impurities unavoidably present in graphene on substrates.[7–9] Such ultrapure graphene (in this article, "graphene" mostly implies "suspended graphene" without any substrates) with ultrahigh mobility is of considerable importance for a number of reasons. First, a careful comparison between graphene experimental data with and those without substrates could teach the community a great deal about the type of disorder operational in graphene on various substrates and the associated scattering mechanisms limiting graphene mobility on substrates,[10] thus helping the eventual technological application of graphene-based devices. Second, ultrapure SG enables the study of interaction effects[6,11–13] without the considerable complications arising from disorder, and additionally, the absence of dielectric screening by the substrate enhances the Coulomb interaction. Third, as a direct consequence of the high sample purity, SG is a convenient system for experimental study of the fractional quantum Hall effect.[2,4] Fourth, the (relative) absence of disorder in SG suppresses the electron-hole puddle formation around the charge-neutrality point, i.e., the Dirac point, making it relatively easier to access the intrinsic Dirac point physics by lowering the carrier density.[5]

The last item ("accessing the Dirac point") along with the first item ("understanding transport in SG") provides the motivation of our theoretical research presented in the current paper, where we carry out a detailed quantitative study of SG carrier transport as a systematic function of temperature and carrier density neglecting all complications arising from the inhomogeneous electron-hole puddles[14–16] in the system (which typically become operational below a typical carrier density $n_c \sim 10^{12}$ cm^{-2} for graphene on SiO_2 substrates).[14,15] Our theoretical results provide a direct estimate of the disorder-limited SG transport properties down to low carrier densities which experiments should be able to access in clean SG samples where inhomogeneous puddle formation is pushed down to very low carrier densities. Our work, therefore, should provide a benchmark for understanding SG transport data as well as for figuring out how close to the Dirac point specific SG experimental samples manage to approach.

A characteristic and universal feature of graphene transport is the minimum conductivity phenomenon where, at some disorder-dependent low carrier density (n_c), the conductivity shows an approximate saturation as a function of the carrier density, forming a rough minimum conductivity plateau around the Dirac point[7–9] with a characteristic electron-hole density width of $\pm n_c$. The characteristic density cutoff n_c defining this minimum conductivity plateau roughly defines how close in density [or in energy $\varepsilon_c \approx \varepsilon_F(n_c) = \hbar v_F \sqrt{\pi n_c}$, where ε_c is the graphene Fermi energy for carrier density n_c, and v_F is the graphene Fermi velocity] the particular graphene sample approaches the Dirac point. The larger the n_c (or E_c), the farther the system is from the Dirac point, no matter how low one tunes the gate voltage since the Dirac point is defined only to the uncertainty of n_c. It is now reasonably well established[8–10,17,18] that the minimum conductivity plateau and the characteristic density cutoff arise from disorder-induced density inhomogeneity (or, equivalently, electron-hole puddle formation) in the system, which makes it impossible to access the Dirac point nominally existing precisely at zero carrier density. Instead the disorder-induced density fluctuations characterized by n_c make the zero-density (and as such, measure-zero) Dirac point ill defined over a scale of n_c. The smaller n_c is, the more closely one can approach the Dirac point by tuning the gate-voltage-induced carrier density. Thus, transport measurements, which probe n_c directly by definition (since for $|n| < n_c$ the conductivity approximately saturates), provide a clear signature for how close to the Dirac point one is able to approach in a particular graphene sample. In high-quality SG, $n_c \sim 10^8$ cm^{-2} can be achieved,[5] indicating that experiments can assess the Dirac point within $\varepsilon_c \sim 0.4$ meV ~ 5 K. With further improvement in SG sample quality, it is conceivable that the SG Dirac point could be accessed within 0.5 K, leading to the possibility of studying

 ©2013 American Physical Society

intrinsic interaction phenomenon associated with the non-Fermi liquid aspects of the Dirac point.[11–13] This Dirac point accessibility is the primary motivation for our detailed current study of SG transport properties as functions of carrier density and temperature. In this work we assume that $n_c = 0$, and our results therefore only apply to ultrapure SG samples at doping densities above the conductivity minima and/or at $k_B T > \varepsilon_c$.

In addition to the Dirac point accessibility issue discussed above, a secondary motivation of our work is a qualitative theoretical understanding of realistic SG transport in order to assess whether the current experimental SG samples are in the ballistic or the diffusive regime. Several recent SG experimental investigations[1–5] conclude that their studied samples are in the ballistic regime based on the estimated transport mean free path being longer than (or comparable to) the linear sample size. Such very long mean free paths imply essentially no carrier scattering within the sample (and, consequently, almost no disorder), and thus the issue of diffusive versus ballistic transport in SG samples is an important topic of considerable interest to the community. We find that this is also a very subtle topic since the extraction of the mean free path from the measured conductivity is quite nontrivial at a low gate voltage (i.e., near the Dirac point) where intrinsic thermal carrier occupancy (because of the zero-band-gap nature of graphene) effects become crucial, and a näive estimate of the mean free path using simply the gate-induced carrier density would seriously overestimate the mean free path. In fact, we believe that at low carrier densities it is much more sensible to discuss the physics simply in terms of the dimensionless two-dimensional (2D) conductivity (in units of e^2/h) rather than in terms of the mean free path and/or mobility, which are both derived by dividing the measured conductivity by a putative carrier density subject to large errors near the charge-neutrality point. We find that a theoretical description based on purely diffusive transport using the semiclassical Drude-Boltzmann theory gives a reasonable description for the experimentally observed SG transport properties. We believe that the only way to definitively establish ballistic SG transport is to experimentally observe the explicit sample-size-dependent conductivity characterizing ballistic transport, where conductance, and not conductivity, is the meaningful physical quantity, which, to the best of our knowledge, has not yet been seen in any SG samples by any experimental group. We therefore contend, based on our theoretical results, that the currently existing SG samples are all high-mobility diffusive samples.

We consider primarily disorder-induced resistive scattering in our theory[10,17,18] since our interest is mainly the issue of approaching the Dirac point in high-quality SG. The phonon effects have been considered elsewhere in detail,[19–22] and it is straightforward to include phonons in the theory; we do provide some results including phonon scattering in the theory since their effect could be important at higher (lower) temperatures (carrier densities).

The rest of this article is organized as follows. In Sec. II we describe our basic transport model and provide the expected theoretical results for finite-temperature Drude transport of intrinsic (i.e., undoped) graphene precisely at the Dirac point, which serves as the starting point for later discussions. In Sec. III we provide our full theory, and then in Sec. IV we provide our numerical results, concluding in Sec. V with a discussion and a summary.

II. INTRINSIC TRANSPORT AT THE DIRAC POINT

Precisely at the Dirac point ($n = 0$), assuming no disorder-induced electron-hole puddles and $T = 0$, it is easy to see that the semiclassical Drude-Boltzmann conductivity σ_D at the Dirac point (or, equivalently, the charge-neutrality point) is precisely 0 (i.e., infinite resistivity) because of the trivial reason that there are no carriers to carry any current. We note that in our zeroth-order Drude-Boltzmann transport theory the matrix element of the off-diagonal terms vanishes due to the conservation of energy, which gives rise to the zero conductivity at $T = 0$ and $n = 0$. But more rigorous transport theories (such as the Kubo formula and the self-consistent Boltzmann transport theory, which are beyond the Boltzmann theory) produce nonvanishing matrix elements between off-diagonal terms even at $n = 0$. Thus the well-known minimum conductivity appears in these theories. Since our analysis is totally based on the zeroth-order Boltzmann theory the conductivity vanishes for $n = 0$ even for chiral graphene. This trivial result is unstable because there will be a finite conductivity the moment the carrier density deviates from the precise measure-zero $n = 0$ constraint, which is bound to happen at $T \neq 0$ even at the Dirac point by virtue of the low-energy thermal electron-hole excitations capable of carrying the current. Unlike ordinary band insulators with finite band gaps,[23] there is no exponential suppression of finite-temperature band conductivity in graphene because of its gaplessness. Instead, as is well-known and discussed in some detail below, $\sigma_D(T)$ at the Dirac point of graphene manifests a power-law "insulating" temperature dependence, which should distinguish the Dirac point behavior from the saturated conductivity behavior in the presence of electron-hole puddles.[18,24] This power-law insulating behavior associated with the Dirac point has nothing to do with Anderson localization physics and arises entirely within the metallic Drude-Boltzmann diffusive transport theory because graphene is a gapless semiconductor.

Consider undoped graphene in the absence of disorder (or electron-hole puddles), i.e., the chemical potential at $T = 0$ lies at the Dirac point. Then the thermally excited number of electrons (and holes) at finite temperatures can be calculated as

$$n = \int D(\varepsilon) n_F(\varepsilon) d\varepsilon, \tag{1}$$

where n_F is the Fermi distribution function and $D(\varepsilon) = g\varepsilon/2\pi\gamma^2$ is the density of states (DOS) of graphene, with the total degeneracy $g = 4$ arising from spin (2) and valley (2)and $\gamma = \hbar v_F$. The induced carrier density at T becomes

$$n = \frac{g}{2\pi}\frac{\pi^2}{12}\frac{(k_B T)^2}{\gamma^2} = T^2 \times 0.89 \times 10^6 \text{ cm}^{-2}. \tag{2}$$

At $T = 300$ K we have $n = 8 \times 10^{10}$ cm^{-2}. Thus if the conductivity is simply proportional to the carrier density, it increases quadratically with temperature. We show below that the actual temperature dependence of the conductivity depends on the scattering mechanism.

In the presence of disorder-induced momentum scattering the conductivity can be calculated within Boltzmann transport theory. In this theory the puddle effect is not considered, i.e., the theory is valid only for $n > n_c$. The conductivity is given by[10,25]

$$\sigma_D(T) = \frac{e^2 v_F^2}{2} \int d\varepsilon D(\varepsilon)\tau(\varepsilon)\left(-\frac{\partial f(\varepsilon)}{\partial \varepsilon}\right), \quad (3)$$

where τ is the disorder-induced transport scattering time. Note that in this equation the conductivity is not related explicitly to the carrier density. If we assume a constant scattering time, i.e., no energy and temperature dependence of the scattering time, then we have

$$\sigma_D(T) = \frac{e^2}{h}\frac{2\ln 2}{\gamma}(\tau_0 v_F)(k_B T), \quad (4)$$

where τ_0 is the constant scattering time and the mean free path is given by $l = \tau_0 v_F$. In this case the conductivity increases linearly with temperature.

Now consider a generalized scattering time. Within the Fermi golden rule we have

$$\frac{1}{\tau} = \frac{2\pi}{\hbar} n_i \sum_{k'} |V_i(k,k')|^2 (1 - \cos\theta_{kk'})\delta(\varepsilon_k - \varepsilon_{k'}), \quad (5)$$

where n_i is the impurity concentration and V_i is the carrier-impurity scattering potential.

For a short-range potential (i.e., δ-range potential) with the strength $V_i = V_\delta$ and the impurity density $n_i = n_\delta$, we have

$$\frac{1}{\tau(\varepsilon)} = \frac{n_\delta V_\delta^2}{4}\frac{v_F \varepsilon}{\gamma^3}. \quad (6)$$

With Eq. (3) we have

$$\sigma_D(T) = \frac{4e^2}{h}\frac{\gamma^2}{n_\delta V_\delta^2}. \quad (7)$$

Thus the conductivity is independent of the temperature for δ-correlated zero-range disorder.

For an unscreened long-range Coulomb potential, $V_i(q) = 2\pi e^2/\kappa q$, where κ is the background lattice dielectric constant (taken to be unity for SG), we have

$$\frac{1}{\tau(\varepsilon)} = \frac{\pi^2}{\hbar} n_i \frac{r_s^2 \gamma^2}{\varepsilon}, \quad (8)$$

where $r_s = e^2/\kappa\gamma$ is the graphene fine-structure coupling constant. With Eq. (3) we have

$$\sigma_D(T) = \frac{e^2}{h}\frac{1}{3n_i}\frac{1}{r_s^2\gamma^2}(k_B T)^2. \quad (9)$$

For a screened long-range Coulomb potential, i.e.,

$$V_i(q) = \frac{2\pi e^2}{\kappa q \epsilon(q)}, \quad (10)$$

where the dielectric function, $\epsilon(q)$, is given by

$$\epsilon(q) = 1 + \frac{2\pi e^2}{\kappa q}\Pi(q,T), \quad (11)$$

and where $\Pi(q)$ is the polarizability depending on the wave vector and temperature,[26] within the RPA we have

$$\Pi(q,T) = \frac{q}{4\gamma} + \frac{4}{\pi\beta\gamma^2}\left[\ln 2 - \int_0^{\beta\varepsilon_q/2} \frac{\sqrt{1-(2y/\beta\varepsilon_q)^2}}{1+e^y} dy\right], \quad (12)$$

where $\beta = 1/k_B T$ and $\varepsilon_q = \hbar v_F q$. Finally, the conductivity can be calculated to be (with some straightforward algebra)

$$\sigma_D(T) = \frac{e^2}{h}\frac{1}{2\pi n_i}\frac{(k_B T)^2}{r_0^2\gamma^2} I(r_0), \quad (13)$$

where

$$r_0 = \frac{r_s}{1 + \pi r_s/2}, \quad (14)$$

and $I(r_0)$ is a function which is independent of the temperature and given by

$$I(r_0) = \int_0^\infty dt\, t^2 \tau(t,r_0)\frac{e^t}{(e^t+1)^2}, \quad (15)$$

where

$$\frac{1}{\tau(t,r_0)} = \int_0^1 dx \frac{\sqrt{1-x^2}}{\epsilon_0(2tx,r_0)^2} \quad (16)$$

and

$$\epsilon_0(z,r_0) = 1 + \frac{4r_0}{z}\left[\ln 2 - \int_0^{z/2} \frac{\sqrt{1-(2y/z)^2}}{1+e^y} dy\right]. \quad (17)$$

Thus the Dirac point conductivity increases quadratically with temperature for a screened Coulomb potential disorder, similar to the bare Coulomb disorder results in Eq. (9).

Finally, for scattering of the thermally excited carriers by deformation potential coupling to acoustic phonons,[19] we get the following expression in the high-temperature nondegenerate equipartition phonon distribution regime:

$$\sigma_{ph} = \frac{e^2}{h}\frac{8\rho_m v_{ph}^2 \gamma^2}{D^2}\frac{1}{k_B T}, \quad (18)$$

where D is the deformation potential, ρ_m the graphene mass density, and v_{ph} the phonon velocity. Thus, the conductivity decreases inverse linearly with increasing temperature. For low temperatures, $T < T_{BG}$, where the T_{BG} is the so-called Bloch-Grüneisen temperature, phonon scattering is very strongly suppressed[19] and is not of any interest in the current work.

We note that, as expected, the above Boltzmann theoretical semiclassical description of the Dirac point conductivity, which neglects all interactions[27] and interference effects[28–30] (but includes thermal excitation, screening, and scattering effects quantum mechanically), gives $\sigma_D(T=0) = 0$ at the Dirac point, and the finite $\sigma_D(T)$ for $T \neq 0$ arises entirely from the finite density of thermal electron-hole excitations [c.f., Eq. (1)] in gapless graphene. The temperature dependence of the finite-temperature Dirac point conductivity is entirely a power law with $\sigma_D(T) \sim T^\alpha$, where $\alpha = 0$, 1, or 2, respectively, depending on whether the scattering mechanism is short-ranged or energy-independent or long-ranged (including screened Coulomb scattering). In addition, $\alpha = -1$ for phonon scattering as shown in Eq. (18), and in the presence of all possible scattering mechanisms, the actual temperature-dependent Dirac point conductivity would be nonuniversal and

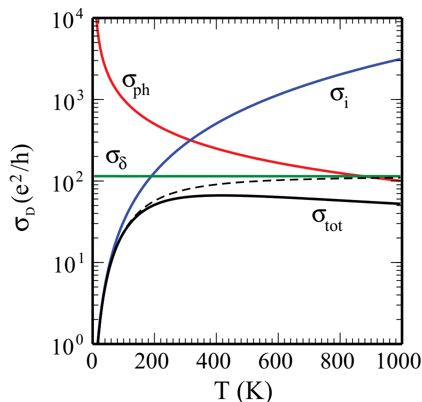

FIG. 1. (Color online) The Dirac point conductivity σ_D as a function of temperature. σ_i (σ_δ) indicates the conductivity due to screened charged Coulomb disorder with an impurity density $n_i = 0.3 \times 10^{10}$ cm^{-2} [short-range disorder with $n_\delta V_\delta^2 = 1.5$ (eV Å)^2]. σ_{ph} represents the conductivity limited by acoustic phonon scattering. σ_{tot} is the total conductivity including all scattering mechanisms. The dashed line indicates the conductivity due to the Coulomb disorder and the short-range disorder.

complex, depending on the strength of the various scattering processes in the particular sample. It is then easy to see that the experimentally measured α exponent could be any number between 0 and 2, depending on the manifestly nonuniversal strength of various scattering mechanisms in the system.

The important point to note is that the temperature dependence is never exponential, a key qualitative feature which helps to distinguish the Dirac point thermally induced conductivity from the Anderson (strong) localization (or gap-induced insulating) behavior. This power-law temperature-dependence feature remains valid even in the presence of phonon scattering which leads to a metallic conductivity (i.e., a negative α) with a temperature-dependent conductivity with a power law between 1 and 5,[19] depending on whether or not the Bloch-Grüneisen regime is relevant. We emphasize that phonons can only induce metallic behavior (with the conductivity decreasing with increasing temperature), and as such, disorder and phonon scattering together may produce a complicated nonmonotonic temperature dependence. In Fig. 1 we show the calculated σ_D including all three scattering mechanisms (i.e., short-range and long-range disorder as well as acoustic phonons). The total conductivity (σ_{tot}) shows a nonmonotonic temperature dependence. As the temperature increases, σ_{tot} increases due to the dominance of Coulomb disorder at low temperatures, but after reaching a maximum conductivity it decreases with increasing temperature due to phonon scattering. This crossover temperature scale for $\sigma_D(T)$ depends sensitively on the amount of Coulomb disorder in the system and increases (decreases) with increasing (decreasing) Coulomb disorder. We note that if Coulomb disorder is weak or absent, $\sigma_D(T)$ decreases monotonically with increasing temperature because of phonon scattering. The fact that experimental low-density SG transport data[1–5] show a nonmonotonic temperature dependence of low-density SG conductivity clearly indicates that Coulomb disorder dominates even the currently existing SG samples (and not just the graphene-on-substrate samples).

A key aspect of the temperature-dependent Dirac point electrical conductivity derived above, which, although rather obvious, has not been much discussed in the literature, is that the intrinsic Dirac point behavior is really a *high-temperature* phenomenon rather than a low-temperature one since one must have $n(T) > n_c$ in order to see the intrinsic behavior (where n_c is the characteristic cutoff density defining electron-hole puddle formation in the system). Thus, the intrinsic Dirac point physics can only be accessed for $T \gg T_c \approx 10^{-3}\sqrt{n_c}$, with $n_c(T)$ measured in units of cm^{-2} (K), and the intrinsic Dirac point behavior is completely suppressed by the extrinsic inhomogeneous carrier density fluctuations associated with electron-hole puddles. For the extremely low value of $n_c \sim 10^8$ cm^{-2}, we get $T_c = 10$ K, whereas for the usual graphene-on-SiO_2 substrates, where $n_c \approx 10^{12}$ cm^{-2}, $T_c \approx 1000$ K! Thus, the intrinsic Dirac point conductivity (and its strongly insulating temperature dependence arising from Coulomb disorder) can never be observed in most graphene-on-SiO_2 samples studied in most laboratories, and indeed, in spite of clear theoretical predictions for the insulating temperature dependence of low-density graphene conductivity,[25] for a long time it was believed that graphene conductivity is essentially temperature independent up to room temperature (since the electron-phonon coupling constant is small in graphene, even phonon-induced metallic temperature dependence is fairly weak in graphene at a high carrier density).

To observe the intrinsic Dirac point physics $\sigma_D(T)$ at low temperatures ($\lesssim$100 mK) so that various predicted interaction-induced Dirac point reconstructions (or instabilities)[13] can be experimentally observed (since higher temperature strongly suppress interaction effects), one would have to produce SG samples of rather extraordinary purity, with the puddle-induced density inhomogeneity being less than 10^4 cm^{-2}. This seems a rather daunting task, and it is therefore safe to say that the $T \to 0$ intrinsic Dirac point conductivity is unlikely to be experimentally explored in the near-future, making our current work, where we consider finite-temperature Dirac point transport neglecting interaction effects, relevant for all experimental Dirac point transport studies in the near-future.

Before concluding this section we emphasize that we are only considering $T \neq 0$ disorder-limited Boltzmann conductivity in our theory, neglecting all interaction effects, and for $T = 0$ our Dirac point conductivity is trivially 0. A completely different approach is necessary to discuss intrinsic Dirac point conductivity in clean graphene at $T = 0$, where interaction and quantum interference effects would be important. Such a theory is beyond the scope of our work and is not of interest to us since we know of no experimental relevance of the $T = 0$ Dirac point conductivity. Second, the inclusion of phonon effects is extremely important for the Dirac point conductivity behavior as a function of temperature since phonons lead to nonmonotonic $\sigma_D(T)$ with metallic behavior ($d\sigma_D/dT < 0$) at higher temperatures, replacing the insulating behavior ($d\sigma_D/dT > 0$) at lower temperatures with a nonuniversal disorder-dependent crossover behavior.

III. CONDUCTIVITY OF SUSPENDED GRAPHENE

Our theoretical model assumes the absence of puddles in the system, and as such, the theory is cut off at some

sample-dependent characteristic carrier density n_c below which the inhomogeneous density fluctuations around the Dirac point become important, leading to an observable minimum-conductivity plateau formation. The theory is valid only for $n \gtrsim n_c$ or in the nonplateau regime by definition. If n_c is very small, as has been claimed in several recent experimental studies,[1–6] then our theory would apply down to very low carrier densities (as long as interference and interaction effects are negligible). Puddle effects on graphene transport properties have been theoretically studied elsewhere,[24] and puddles would introduce additional nontrivial temperature and density dependence for $n \lesssim n_c$, which is not of interest to us in the current work, where n_c is very small by virtue of the ultraclean nature of SG in general.

In our theory, we consider three distinct scattering mechanisms contributing to the SG resistivity. These are charged impurity, short-range disorder, and in-plane acoustic phonon scattering processes. There can be other types of scattering mechanisms contributing to the graphene resistivity such as resonant scattering centers,[31,32] ripples,[33] and flexural phonons.[34–36] The short-range disorders considered in the resonant scatterers[31,32] modify the DOS of graphene (i.e., there is a resonant DOS peak at the Dirac point due to these disorders). In this case short-range disorder scattering gives rise to density-dependent conductivity. In our Boltzmann theory, to keep the theory consistent for all other disorders we used the bare DOS of pure graphene and we obtained the density-independent conductivity from the short-range disorder. In this paper the short-range disorder represents the zero-range disorder, i.e., $V(r) = V_\delta \delta(r)$. The calculated scattering time with the finite-width potential [i.e., $V(r) = V_\delta \theta(r - r_0)$] does not significantly modify that with the zero-range potential as long as $r_0 < 2a$, where a is the lattice constant of graphene. In SG the flexural phonons may dominate the phonon contribution to the resistivity.[35,36] However, in SG under specific tension induced by contacts (this is the case for all available SG samples) the flexural phonon contribution to the conductivity is severely suppressed, and as a consequence the in-plane phonon is the dominant scattering mechanism.[36] Since we consider SG under tension our calculated results are not affected by the flexural phonons. The possibility of still other unknown scattering mechanisms (such as scattering from the hybridization of electron-hole excitations and out-of-plane optical phonons)[37] contributing to the graphene resistivity cannot be ruled out either. But we neglect these scattering mechanisms because we want to keep the number of parameters to a minimum and also because the very high SG mobility and quality imply that the overall scattering contributions are small.

The Drude-Boltzmann conductivity theory for extrinsic graphene in the presence of induced carriers is a straightforward generalization of the theory provided in Sec. II except the total carrier density now has an externally tunable (through the gate voltage) density in addition to the thermally excited intrinsic carriers considered in Sec. II. This theory has been much discussed in the literature, and we provide below the working equations for different contributions to the SG resistivity from the three scattering mechanisms considered in our work. The theory below is a straightforward generalization of the theory for the finite-temperature Dirac point conductivity developed in Sec. II.

Within the Boltzmann transport theory,[10,25] the conductivity $\sigma(n,T)$ is given within the relaxation time approximation by

$$\sigma = \frac{e^2}{2}\int d\epsilon\, D(\epsilon) v_k^2 \tau(\epsilon)\left[-\frac{\partial f(\epsilon)}{\partial \epsilon}\right], \tag{19}$$

where $f(\epsilon)$ is the relevant distribution function. The relaxation time $\tau(\epsilon) \equiv \tau(\epsilon_k)$ is given after ensemble averaging over a random disorder configuration by

$$\frac{1}{\tau^{(\alpha)}(\epsilon_k)} = \frac{2\pi}{\hbar}\sum_{(\alpha)} n_i^{(\alpha)} \int \frac{d^2k'}{(2\pi)^2} \left|\langle V_{kk'}^{(\alpha)}\rangle\right|^2 \times (1-\cos\theta_{kk'})\delta(\varepsilon_k - \varepsilon_k'), \tag{20}$$

where $\theta_{kk'}$ is the scattering angle and $V^{(\alpha)}$ is the potential disorder causing the scattering, with $n_i^{(\alpha)}$ being the 2D density of the random impurities (or defects) producing the disorder and (α) being a label indicating the kind of scatterer (e.g., long-range Coulomb scattering, short-range defect scattering, etc.) under consideration, with each scattering mechanism being independent.

The finite-temperature conductivity is given by an appropriate thermal energy averaging within the Boltzmann theory once $\tau(\epsilon)$ has been calculated. The zero-temperature result is simply given by

$$\sigma = \frac{e^2 v_F^2}{2} D(\epsilon_F)\tau(\epsilon_F), \tag{21}$$

where the graphene Fermi velocity v_F is assumed to be a constant (independent of momentum and density) and ϵ_F, the Fermi energy, is the chemical potential at $T = 0$. The finite temperature chemical potential, $\mu(n,T)$, is calculated self-consistently[25] so that the net carrier density (induced by doping or an external gate) is n, and the gaplessness of graphene automatically ensures that this procedure incorporates the thermally excited carriers (i.e., the only carriers present for intrinsic graphene as considered in Sec. II at the Dirac point with $\epsilon_F = 0$) along with the induced carriers of density n. In this paper our main interest is the low-carrier-density regime where n is small so that the Dirac point behavior is accessed.

A. Short-range disorder

For short-range (or, more appropriately, zero-range) δ scatterers, we have

$$|\langle V_{kk'}\rangle|^2 = V_\delta^2(1+\cos\theta)/2, \tag{22}$$

where V_δ is the strength of the short-range disorder and the $(1+\cos\theta)/2$ factor arises from the matrix elements effect due to the pseudospin chirality of graphene (this chirality factor leads to the famous suppression of back scattering in graphene and also in surface states of topological insulators).

It is easy to show that short-range disorder leads to a carrier-density-independent conductivity $\sigma(n) \propto V_\delta^{-2}$ and to an exponentially suppressed temperature dependence at low temperatures. In the high-temperature limit, the resistivity due to short-range disorder increases by a factor of 2 compared with the $T = 0$ value,[25] and thus, short-range disorder by itself introduces weak metallic behavior in graphene with little temperature dependence at low ($T \ll T_F = \epsilon_F/k_B$) temperatures and increasing resistivity at high temperatures

($T \to \infty$). This is the same thing that happens to just the Dirac point conductivity as discussed in Sec. II.

B. Long-range Coulomb disorder

Unintentional charged impurity centers in the environment are a major source of disorder for graphene on substrates. Although they are substantially removed in annealed SG samples (leading to the very high observed SG mobility), there are still some remnant random charged impurity centers on the SG surface which contribute to carrier scattering. For Coulomb disorder we have

$$|\langle V_{kk'} \rangle|^2 = \left| \frac{V_c(q)}{\epsilon(q)} \right|^2 \frac{1+\cos\theta}{2}, \tag{23}$$

where $V_c(q) = 2\pi e^2/\kappa q$, with κ (=1 for SG) as the background dielectric constant, is the 2D Coulomb interaction and $\epsilon(q)$ is the wave-vector-dependent static dielectric function of the free carriers in graphene.[10,17]

The density dependence $\sigma(n)$ of conductivity due to Coulomb disorder is linear, $\sigma \sim n$, and the preponderance of the observed linearity of $\sigma(n)$ on n is considered to be strong evidence for the importance of charged impurity scattering in determining graphene transport properties. The temperature dependence due to Coulomb disorder has been discussed elsewhere,[25] and here we summarize the main findings for the discussion of our results presented in the rest of this paper. In the low-temperature limit ($T \ll T_F = \epsilon_F/k_B$), one gets for Coulomb disorder

$$\sigma(T) = \sigma_0[1 - A_2(T/T_F)^2], \tag{24}$$

where $A_2 > 0$. In the high-temperature limit ($T \gg T_F$), which is the more appropriate regime for our consideration of transport near the Dirac point ($n \sim 0$), one gets

$$\sigma(T) \sim B_2(T/T_F)^2, \quad \text{with} \quad B_2 > 0. \tag{25}$$

Thus, Coulomb disorder by itself predicts weak metallic behavior for $T \ll T_F$ and strong insulating behavior for $T \gg T_F$ (which is the appropriate limit for the low-density Dirac point regime).

C. Acoustic phonon scattering

In addition to short-range and long-range disorder, which affect the SG conductivity at all temperatures (but with distinct density and temperature dependence in different regimes), we also include resistive scattering by graphene acoustic phonons through deformation potential coupling, which is operational primarily at higher temperatures (except at the Dirac point, where it is operational at all temperatures). We note that the deformation potential coupling is rather weak in graphene, and therefore, the primary (essentially, the only) effect of phonon scattering is to introduce a weak metallic temperature dependence on the phonon-induced resistivity $\rho_{\rm ph} \sim T$ at higher temperatures $T > T_{\rm BG} \sim 2\hbar v_{\rm ph} k_F$, where $v_{\rm ph}$ is the phonon velocity (i.e., speed of sound). Since $k_F \propto \sqrt{n}$, phonon effects could affect the net SG resistivity at fairly low temperatures for the low-carrier-density systems of our interest in this work. Since k_F effectively vanishes at the Dirac point, acoustic phonons are operational even at arbitrarily low temperatures near the Dirac point as $T_{\rm BG}$ tends toward 0.

Since phonon scattering has already been considered in detail theoretically elsewhere,[19] we show below the relevant "high-temperature" relaxation time for the deformation potential coupling,

$$\frac{1}{\tau(\epsilon)} = \frac{1}{\hbar^3} \frac{\epsilon}{4v_F^2} \frac{D^2}{\rho_m v_{\rm ph}^2} (k_B T), \tag{26}$$

where D and ρ_m are, respectively, the deformation potential coupling and graphene mass density. At very low temperatures, the phonon-induced relaxation time enters the Bloch-Grüneisen regime where $\rho_{\rm ph} \sim T^4$ and is negligibly small.[19] In our numerical results presented later in this paper, we use the full numerical solution of the Boltzmann theory for calculating the phonon-induced resistivity, which always becomes important above (a density-dependent) a characteristic temperature.

D. Asymptotic behavior of SG conductivity

We now combine the contributions to $\sigma(T,n) = [\rho(T,n)]^{-1}$ from the three distinct scattering mechanisms described in Secs. III A–III C to discuss the asymptotic density and temperature dependence of SG conductivity near the Dirac point. First, we establish the counter-intuitive result that the conductivity around the Dirac point is always affected by phonon scattering even at arbitrarily low temperatures. Writing the effective carrier density $n(T)$ around the Dirac point as

$$n(T) \approx n_0 + AT^2, \tag{27}$$

where $n_0 \propto V_g$ is the gate-induced extrinsic carrier density and AT^2 ($\gg n_0$) is the intrinsic Dirac point thermally excited carrier density (see Sec. II), we can define an effective Fermi wave vector,

$$k_F = \sqrt{\pi(n_0 + AT^2)} \approx \sqrt{\pi A} T, \tag{28}$$

where $A = (\pi/6)(k_B/\gamma)^2$ are known T-independent constants. Then the Bloch-Grüneisen temperature $T_{\rm BG}$ above which phonon scattering effects are important is given by

$$T_{\rm BG} = \omega_{\rm ph}(2k_F)/k_B = 2(v_{\rm ph}/v_F)\sqrt{\pi^2/6}T = dT, \tag{29}$$

where $d = 2v_{\rm ph}/v_F\sqrt{\pi^2/6}$. (We note that $T_{\rm BG}$ is defined by phonons with an effective wave vector of $2k_F$ since $2k_F$ typically is the most resistive scattering process across the Fermi surface.) Now the condition for acoustic phonons to contribute appreciably to the resistivity (e.g., $\rho \propto T$) is that $T > T_{BG}$, implying that $d > 1$. If $d > 1$, then the Dirac point resistivity remains unaffected by phonons to arbitrarily high temperatures, whereas $d < 1$ implies that phonons contribute a linear resistivity down to low temperatures. It is easy to check that for actual graphene parameters, we find that $d \approx 10^{-3}$ and thus $d \ll 1$ is satisfied, implying that $\sigma_D(T)$ is affected, in principle, by phonon scattering at all temperatures. We can estimate the crossover temperature scale T_c for a low-density SG system to go from being "insulating-like," dominated by Coulomb disorder, to being "metallic-like," dominated by phonon scattering, to be $T_c \sim 2/(A_c B_p)^{1/2}$, where A_c is the coefficient for the T^2 dependence due to Coulomb disorder in

Eq. (13) and B_p is the coefficient of the linear T-inverse term due to phonon scattering in Eq. (18). It is easy to show that $T_c \sim n_i^{1/3}$, and thus the crossover temperature increases with increasing Coulomb disorder in the system. For very pure SG samples, T_c could be very low, and it is, in principle, possible for the low-temperature Dirac point conductivity to show a transition from being insulating-like to being metallic-like as a function of decreasing disorder (i.e., n_i), but this is by no means a localization transition—it is simply a crossover behavior driven by the competition between charged impurities and phonons. In general, the Dirac point conductivity would show complex nonmonotonic temperature-dependent conductivity as is obvious from this analysis and from Fig. 1.

For finite doping when $n_0 \gg AT^2$, the above argument does not hold, and phonon effects on conductivity are pushed to much higher temperatures, while at the same time the temperature scale for the insulating behavior is substantially suppressed since T_F is now large [see Eqs. (24) and (25)]. Then the high-temperature behavior of $\sigma(T)$ must always reflect the weak metallic ($d\sigma/dT < 0$) conductivity in the $\rho_{\rm ph} \propto T$ regime for $T \gg T_{\rm BG}$. Thus, at a high carrier density both the insulating and the metallic temperature dependences are strongly suppressed, leading to a very weak temperature dependence of graphene conductivity as is well established experimentally. How high in temperature one must go to manifest this weak metallic phonon-induced conductivity obviously depends on the gate-induced carrier density. First, $T_{\rm BG}$ increases with increasing carrier density n since $T_{\rm BG} \propto \sqrt{n}$. Thus, doped SG with a high carrier density should reflect a very weak temperature dependence except for the weak phonon-induced metallic behavior at high temperatures, whereas Dirac point conductivity (or, more generally, low-temperature conductivity) should reflect a strong (and, in principle, nonmonotonic) temperature dependence of the conductivity. The observation of any strong temperature dependence in graphene (insulating, metallic, or nonmonotonic) therefore indicates Dirac point behavior.

For short-range disorder, as discussed in Sec. III A, $\sigma(T)$ has a weak T dependence at low temperatures and a metallic temperature dependence at high temperatures, and thus adding phonon scattering does not change the picture qualitatively. Thus, pure short-range disorder by itself can only introduce weak metallic temperature dependence in graphene transport properties, with $\sigma(T)$ decreasing with increasing T at high temperatures as phonons start playing a role. In addition, short-range disorder does not manifest any density dependence of $\sigma(n)$, and therefore, $\sigma(T,n)$ would have little dependence on density and temperature (except at high temperatures) if the dominant resistive scattering mechanism is short-range defect scattering, in conflict with all existing experiments.

Long-range disorder, however, must dominate low-density transport since $\rho \propto 1/n$ for long-range disorder, and therefore, the Dirac point conductivity is necessarily limited by long-range disorder, which, as discussed in Sec. III B, leads to a nonmonotonic temperature dependence of weak metallic behavior for higher temperatures. At low carrier densities (as well as in the presence of any remnant puddles) the low-temperature weak metallicity may be ignored, and the net temperature dependence arising from long-range disorder (Sec. III B) and phonon scattering (Sec. III C) can be combined to give

$$\rho(T) = (\sigma_0 + A_c T^2)^{-1} + B_p T, \tag{30}$$

where σ_0 subsumes the weak metallic temperature dependence at low temperatures and A_c and B_p (as defined above) depend, respectively, on the long-range Coulomb scattering and acoustic phonon scattering as discussed above. For small σ_0, at the Dirac point, such a T dependence leads immediately to a universal crossover temperature scale T_c given by

$$T_c \approx (AB)^{-1/3} \propto n_i^{1/3} r_s^{2/3} v_F^{4/3} v_{\rm ph}^{1/3} D^{-2/3}, \tag{31}$$

with T_c being the characteristic temperature defining the crossover from the temperature power-law insulating temperature dependence induced by Coulomb scattering to the higher temperature phonon-induced weak metallic temperature dependence. We note that T_c increases weakly with disorder (n_i) and r_s but decreases with increasing deformation potential coupling. Cleaner SG systems would thus manifest stronger phonon effects. But for high densities, when σ_0 typically is large, and the phonon effects can only show up at very high temperatures $T \gg T_{\rm BG}(\sim n_0)$, with $T_{\rm BG}$ also being large, Eq. (30) immediately implies very little temperature dependence, except for $\rho(T) \sim T$ for $T \gg T_{\rm BG}$. Thus, away from the Dirac point, whence both T_F and $T_{\rm BG}$ are large, SG conductivity should manifest a weak temperature dependence, whereas the observation of a strong temperature-dependent conductivity is evidence of approaching the Dirac point in the system.

In the next section, we provide our calculated numerical results for SG transport properties using the full numerical solutions of the Boltzmann transport theory including long-range and short-range disorder and acoustic phonon scattering.

IV. NUMERICAL TRANSPORT RESULTS FOR SUSPENDED GRAPHENE

We consider three scattering mechanisms in calculating the density- and temperature-dependent SG conductivity $\sigma(n,T)$ or, equivalently, the resistivity $\rho \equiv 1/\sigma$: long-range Coulomb disorder (n_i), short-range disorder ($n_\delta V_\delta^2$, where n_δ is the short-range impurity density and V_δ is the strength of the short-range disorder), and acoustic phonon scattering (D). We assume $D = 19$ eV throughout and assume that the long-range and the short-range disorder can both be taken to arise from random quenched point impurity centers located in the SG layer.

In addition to conductivity (or resistivity) we also present results for the mobility μ and the mean free path l since these are quantities of considerable experimental interest. In particular, the mean free path is often used by experimentalists to operationally determine whether or not transport is ballistic; if $l > L$ (where L is the system size), one nominally has ballistic transport (and our theory becomes inapplicable). Similarly, mobility is an important physical quantity pertaining to the sample quality; typically SG samples should have a high mobility because the amount of disorder is suppressed.

In calculating the conductivity of extrinsic SG in the presence of finite doping (or gate-induced carriers with a finite Fermi energy ϵ_F) we first generalize the theory of Sec. II to the finite-doping case as discussed below (with n_0 being the doping density). The current density in the presence of an

applied electric field (E_x) is given by

$$J_x = E_x \frac{e^2 v_F^2}{2} \int D(\varepsilon)\tau(\varepsilon)\left(-\frac{df(\varepsilon)}{d\varepsilon}\right)d\varepsilon, \quad (32)$$

where $D(\varepsilon) = g\varepsilon/[2\pi(\hbar v_F)^2]$ is the DOS of graphene with energy $\varepsilon = \hbar v_F k$ and $f(\varepsilon)$ is the Fermi distribution function. Thus the conductivity becomes

$$\sigma = \frac{e^2 v_F^2}{2} \int D(\varepsilon)\tau(\varepsilon)\left(-\frac{df(\varepsilon)}{d\varepsilon}\right)d\varepsilon. \quad (33)$$

To find a direct analogy of the conductivity with the parabolic dispersion, $\sigma = ne^2\langle\tau\rangle/m$, we rewrite Eq. (33) as

$$\sigma(T) = e^2\langle\tau\rangle \frac{g\varepsilon(T)}{4\pi\hbar^2}, \quad (34)$$

where

$$\langle\tau\rangle = \frac{\int D(\varepsilon)\tau(\varepsilon)\left(-\frac{df(\varepsilon)}{d\varepsilon}\right)d\varepsilon}{\int D(\varepsilon)\left(-\frac{df(\varepsilon)}{d\varepsilon}\right)d\varepsilon}, \quad (35)$$

which is exactly the same definition of the average scattering time for 2D parabolic band systems and $\varepsilon(T)$ is given by

$$\varepsilon(T) = \int f(\varepsilon)d\varepsilon = \mu_0(T) + \frac{1}{\beta}\ln[1 + e^{-\beta\mu_0}], \quad (36)$$

where $\mu_0(T)$ is the chemical potential, and at $T = 0$ $\mu_0 = \varepsilon_F$. With the 2D parabolic energy dispersion $\varepsilon = (\hbar k_F)^2/2m$ Eq. (34) becomes the 2D conductivity formula, $\sigma = ne^2\langle\tau\rangle/m$.

With the classical average velocity $\langle v_x\rangle$ the current density is given by

$$J_x = n(T)e\langle v_x\rangle, \quad (37)$$

where we use the total electron density at finite T instead of the zero-temperature density n_0, and $n(T)$ is given by

$$n(T) = \int D(\varepsilon)f(\varepsilon)d\varepsilon. \quad (38)$$

From Eqs. (32) and (37) we have

$$\langle v_x\rangle = \frac{\sigma(T)}{en(T)}E_x. \quad (39)$$

Then the mobility can be defined by (we note that we have used the standard notation μ to imply both mobility and chemical potential, which should not cause any confusion since they do not arise in the same equation in the text and it should be clear from the context whether mobility or chemical potential is being discussed)

$$\mu(T) = \frac{\langle v_x\rangle}{E_x} = \frac{\sigma(T)}{en(T)}. \quad (40)$$

Now we define the mean free path from the average scattering time as

$$l(T) = v_F\langle\tau\rangle = \sigma\frac{h}{e^2}\frac{2}{g}\frac{\hbar v_F}{\varepsilon(T)}. \quad (41)$$

For the mobility [Eq. (40)] and mean free path [Eq. (41)] the total density and thermal energy at finite temperature are used

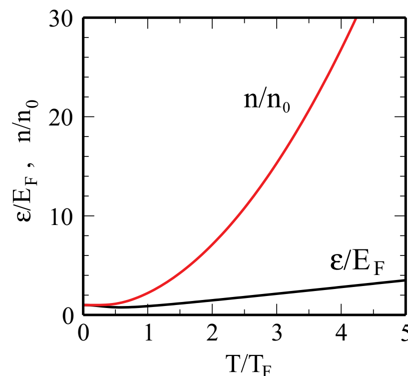

FIG. 2. (Color online) Temperature-dependent electron density $n(T)$ [Eq. (38)] and energy $\varepsilon(T)$ [Eq. (36)] as a function of temperature, T/T_F.

instead of n_0 and ε_F, i.e.,

$$\mu(T) = \frac{\sigma(T)}{en_0} \quad (42)$$

and

$$l(T) = \sigma\frac{h}{e^2}\frac{2}{g}\frac{\hbar v_F}{\varepsilon_F}. \quad (43)$$

We note, as mentioned already, that there are two possible alternative definitions above for the mobility μ and mean free path l, depending on whether one uses the gate-induced doping density n_0 or the full carrier density $n(T)$ including the thermally excited carriers. For $T < T_F$, where T_F $(=\epsilon_F/k_B)$ is always defined with respect to the $T = 0$ carrier density induced by the gate, the two definitions are equivalent since $n(T) \approx n_0 = n$. But at very high temperatures (or very low doping densities), $n(T) \gg n_0$ because $T \gg T_F$. For ordinary graphene on substrates, where the puddle-induced density inhomogeneity introduces a cutoff density of $n_c \sim 10^{12}$ cm^{-2} with a corresponding $T_F \sim 1250$ K, by definition $n(T) = n_0 = n$, and there is not much of a difference between the two different ways of defining the mobility and the mean free path. But for SG, where n_c is small and thus very small values of n_0 are meaningful, the two distinct ways of defining μ and l make a big difference for a low external doping density ($n_0 \sim 0$), i.e., near the Dirac point.

To make the above point more explicit, we show in Fig. 2 our calculated $n = n(T)$ and $\varepsilon(T)$ compared with n_0 and ε_F, respectively. It is clear that for $T/T_F \gtrsim 1$, there is a substantial difference between $n(T)$ and $n_0 = n(T = 0)$. Since $T_F \sim 12$ K for $n_0 \sim 10^8$ cm^{-2}, close to the Dirac point, the two quantities (n and n_0) may differ a lot even at moderate temperatures.

In Figs. 3–10, we show our calculated SG transport properties as functions of density and temperature, neglecting all effects of density inhomogeneity or puddles; our theory should therefore be cut off at some very low doping density ($\lesssim 10^9$ cm^{-2}) where puddles become relevant in high-quality SG. In Figs. 3–8, we show the density dependence for a few representative temperatures, whereas in Figs. 9 and 10 we show the calculated temperature dependence for a few fixed doping densities. We include phonon effects only in Figs. 9 and 10 since our main interest is low-temperature transport. In obtaining our numerical results, we focus on three published

experimental SG works in the literature: Bolotin *et al.*,[3,4] Du *et al.*,[1,2] and Mayorov *et al.*[5] Our goal is not data fitting or getting precise agreement with the experimental results, since the details of disorder are unknown in experimental systems, and we cannot rule out the possibility of additional scattering mechanisms not included in our model being operational in experimental systems. What we are interested in is obtaining the broad qualitative features of SG transport data in our theory in order to critically assess the issues of ballistic versus diffusive SG transport and the access to the Dirac point at a low carrier density. We mention that the authors of all three of these works[1–5] interpret their data in terms of ballistic transport mainly by comparing their extracted mean free paths with the sample size. We critically examine the nature (ballistic or diffusive) of transport in these experiments.

For each experiment, we choose a set of disorder parameters as shown below based on the best overall semiquantitative and qualitative agreement with the data, keeping these disorder parameters fixed for all the presented results. The acoustic phonon scattering parameters are standard and are taken to be $D = 19$ eV, $\rho_m = 7.6 \times 10^{-8}$ g/cm^2, and $v_{\rm ph} = 2 \times 10^6$ cm/s. We use the following disorder parameters for each experiment.

$$\text{Du et al.:}\ \ n_i = 6.5 \times 10^{10}\ \text{cm}^{-2}, \quad n_\delta V_\delta^2 = 15.7\ (\text{eV Å})^2.$$

$$\text{Bolotin } et\ al.\text{:}\ \ n_i = 1.2 \times 10^{10}\text{cm}^{-2}, \quad n_\delta V_\delta^2 = 1.5(\text{eV Å})^2.$$

$$\text{Mayorov } et\ al.\text{:}\ \ n_i = 0.3 \times 10^{10}\text{cm}^{-2},\ n_\delta V_\delta^2 = 1.5\ (\text{eV Å})^2.$$

We note that, consistent with the experimental SG sample quality, our disorder is the strongest (weakest) of Du (Mayorov), with Bolotin disorder being intermediate. This is consistent with the claimed high-density mobility being ∼500 000, ∼200 000, and ∼100 000 cm^2/V s, respectively, in the three experiments (although the precise value of the sample mobility may not be a meaningful quality since the mobility depends on both density and temperature).

In Figs. 3—5, we show our calculated $\sigma(n)$, $\mu(n)$, and $l(n)$ as a function of the doping density n (alluded to n_0 above) for $T = 0$, 100, 200, and 300 K for the three experimental SG samples, respectively. We emphasize that for small values of n_0, where the $T/T_F > 1$ condition may apply, the alternative definitions for the chemical potential and the mean free path would lead to large quantitative differences since, as is obvious from Fig. 2, $n(T) \gg n_0$ in this regime.

Our calculated $\sigma(n)$ results for the three experimental samples in Figs. 3–5 manifest similar qualitative behavior with large quantitative differences because of the differences in the details of the underlying disorder. In particular, the following salient features of the results are consistent with the experimental findings in high-quality SG samples. (i) $\sigma(n)$ manifests sublinear density dependence, simulating $\sigma \sim \sqrt{n}$, over an extended density range and, thus, calling into question the experimental interpretation of SG transport being ballistic[38] based entirely on this sublinear density dependence. (ii) At the lowest density, $\sigma(n)$ is always limited by the long-range Coulomb scattering (with $\rho \propto n$), but the competition between long-range and short-range disorder (which leads to the effective sublinear density dependence over an extended density range) and the existence of the

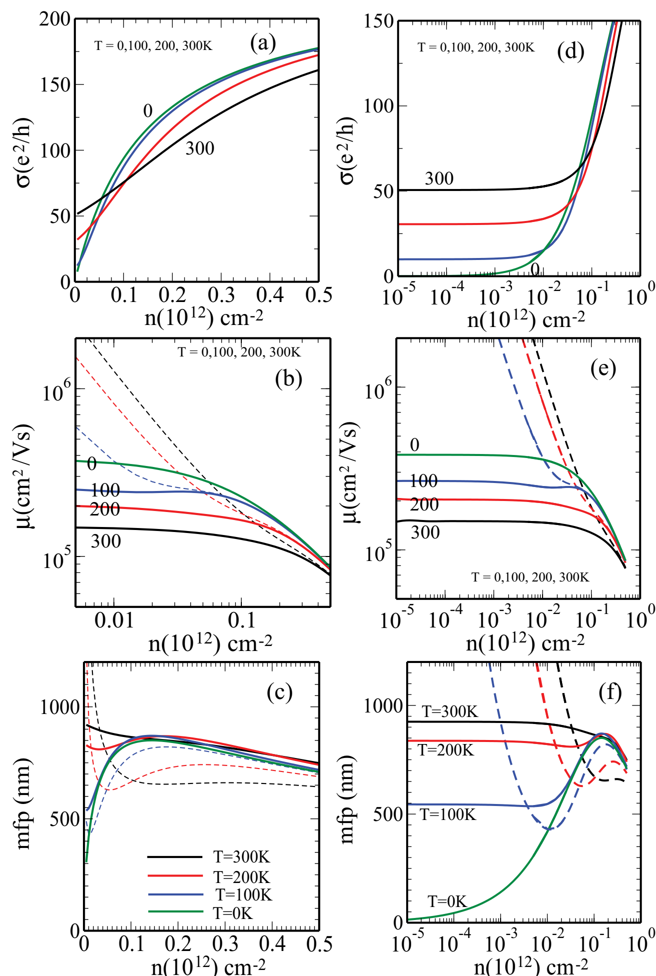

FIG. 3. (Color online) Conductivity of SG corresponding to the experimental data of Bolotin *et al.*[3] (a) Calculated conductivity as a function of density for different temperatures—$T = 0$, 100, 200, and 300 K (from top to bottom)—with $n_i = 0.85 \times 10^{10}$ cm^2 and $n_\delta V_\delta^2 = 1.5$ (eV Å)^2. (b) Mobility and (c) mean free path. Solid lines are calculated with temperature-dependent $n(T)$ and $\varepsilon(T)$, and dashed lines are calculated with the zero-temperature density n_0 and energy E_F. (d) σ, (e) μ, and (f) l at low densities (down to $n = 10^7$ cm^{-2}). Note that as $n \to 0$ or $T/T_F \to \infty$ for a fixed temperature, $\mu(T) \propto \sigma(T)/T^2$ and $l(T) \propto \sigma(T)/T$. Thus, both $\mu(n \to 0)$ and $l(n \to 0)$ saturate at a finite temperature.

low-density puddle-dependent cutoff (not included in the current theory) may mask this linear density dependence in high-quality SG samples where random charged impurity disorder is presumably rather low. (iii) At the lowest density, the system would always manifest insulating temperature dependence because of the dominance of thermal excitation in the gapless system [this is obvious in Figs. 3(d), 4(d), and 5(d)] near the Dirac point—there is a density-dependent crossover to the metallic behavior at higher carrier densities, emphasizing that the characteristic Dirac point insulating transport behavior is a high-temperature crossover behavior (which may not be apparent for $T/T_F \ll 1$. (iv) The calculated mobility approaches ∼5×10^5, ∼5×10^5, and ∼5×10^6 cm^2/V s, respectively, in the Bolotin, Du, and Mayorov samples close to the Dirac point, showing the unprecedentedly high qualities

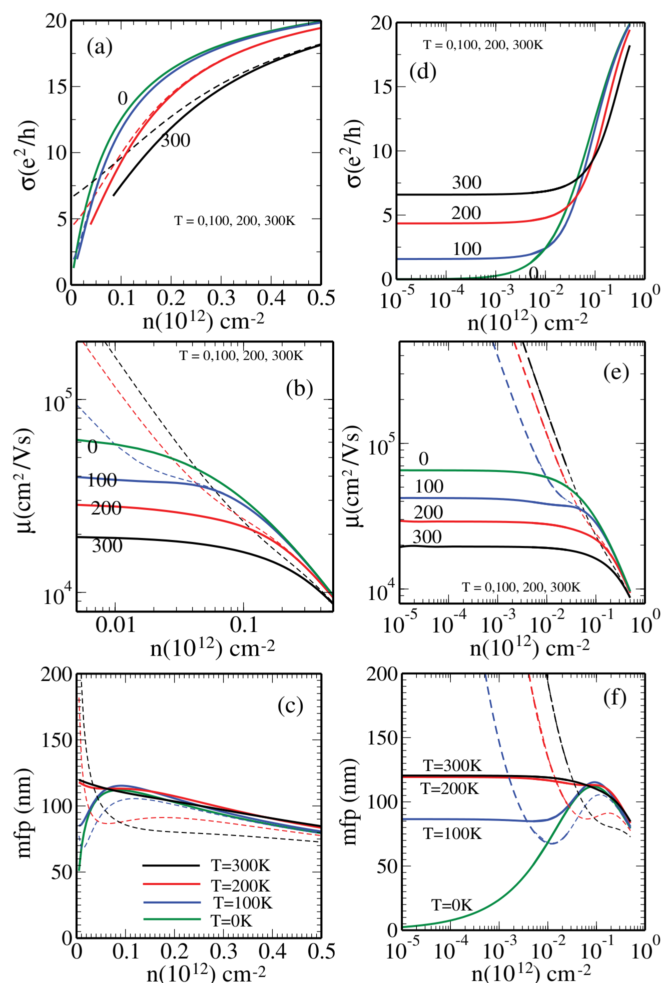

FIG. 4. (Color online) Conductivity corresponding to the experimental data of Du *et al.*[2] (a) Calculated conductivity as a function of density for different temperatures—$T = 0$, 100, 200, and 300 K (from top to bottom)—with $n_i = 5.0 \times 10^{10}$ cm^2 and $n_\delta V_\delta^2 = 14.7$ (eV Å)^2. (b), (c) Mobility (b) and mean free path (c) are shown as a function of density, respectively. Solid lines are calculated with the temperature-dependent $n(T)$ and $\varepsilon(T)$, and dashed lines are calculated with a zero-temperature density n_0 and an energy E_F. (d) σ, (e) μ, and (f) l at low densities.

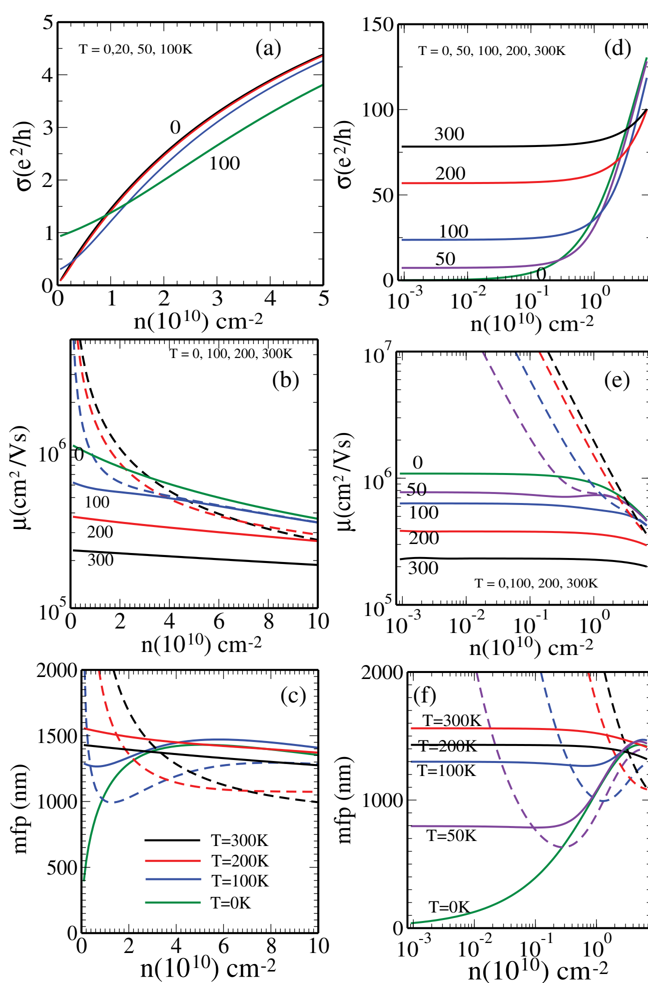

FIG. 5. (Color online) Conductivity corresponding to the experimental data of Mayorov *et al.*[5] (a) Calculated conductivity as a function of density for different temperatures—$T = 0$, 100, 200, and 300 K (from top to bottom)—with $n_i = 0.3 \times 10^{10}$ cm^2 and $n_\delta V_\delta^2 = 1.5$ (eV Å)^2. (b), (c) Mobility (b) and mean free path (c) as a function of density. Solid lines are calculated with the temperature-dependent $n(T)$ and $\varepsilon(T)$, and dashed lines are calculated with a zero-temperature density n_0 and an energy E_F. (d) σ, (e) μ, and (f) l at low densities.

of these SG systems. (v) It is misleading to characterize the mobility (or the mean free path) using the gate-induced density since this would produce an erroneously large mobility and mean free path at low gate voltages and, in fact, would imply a divergent mobility (or mean free path) at the Dirac point—when the full density $n(T)$ is used in defining the mobility (or mean free path), the low-density mobility and mean free path saturate, providing the correct characterization. (vi) Both definitions [using n_0 or $n(T)$] give identical mobility and mean free path values for high carrier densities ($\gtrsim 10^{12}$ cm^{-2}), as one expects, since $n(T) \sim n_0$ for high densities. (vii) Although broadly in qualitative agreement with the experimental data, there are important discrepancies between our theory and experiment in the details, most likely because of our neglect of other possible scattering mechanisms in the experimental systems. (viii) The appropriate mean free path (at low densities near the Dirac point) varies between $\sim$100 nm (Du sample) and $\sim$1000 nm (Mayorov sample), and therefore true ballistic transport measurements would require a sample size of <0.1 μm, and one must observe sample-length-dependent conductivity to validate any ballistic transport behavior.

Since long-range and short-range disorders affect $\sigma(n,T)$ qualitatively differently (and the nature of the disorder in the experimental samples is not known based on any independent measurements), we depict in Figs. 6–8 the distinct theoretical dependence of the conductivity on long-range and short-range disorder separately (in contrast to Figs. 3–5, where both are included together in the theory) on the density for the SG system. To bring out the qualitatively different dependence of conductivity, mobility, and mean free path on n_0 (the doping density) or $n(T)$ at a low density, we show in Figs. 6–8 the dependence on both n_0 and $n(T)$ separately. In Fig. 6, we show the calculated conductivity, whereas in Figs. 7 and 8 we

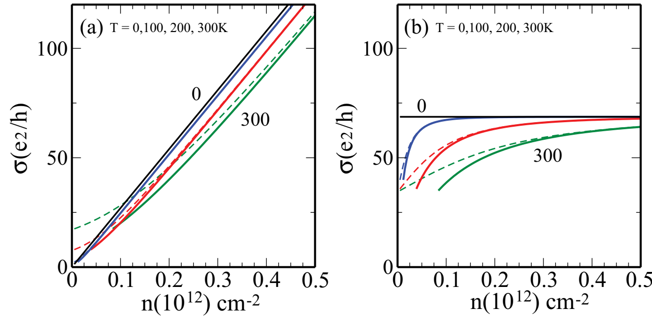

FIG. 6. (Color online) Calculated conductivity as a function of density for different temperatures: (a) For a long-range Coulomb potential with $n_i = 10^{10}$ cm^{-2} and (b) for a neutral short-range potential with $n_\delta V_\delta^2 = 5$ (eV Å)^2. Solid lines indicate σ vs $n(T)$, and dashed lines indicate σ vs $n_0 = n(T = 0)$ or density induced by only the gate voltage.

show the mobility and the mean free path. In Fig. 6 we show $\sigma(n)$ for just long-range disorder or just short-range disorder, with the two different density dependences [n_0 and $n(T)$] showing quantitative differences only at low values of n (or, equivalently, high values of T), with the two being identical (by definition) at $T = 0$ since $n(T = 0) \equiv n_0$. In Figs. 7 and 8, we show the calculated mobility and mean free path for long-range (Fig. 7) and short-range (Fig. 8) disorder with each case also providing the dependence on n_0 and $n(T)$. The important qualitative conclusion from Figs. 6–8 is that one should always extract mobility and mean free path using the correct total

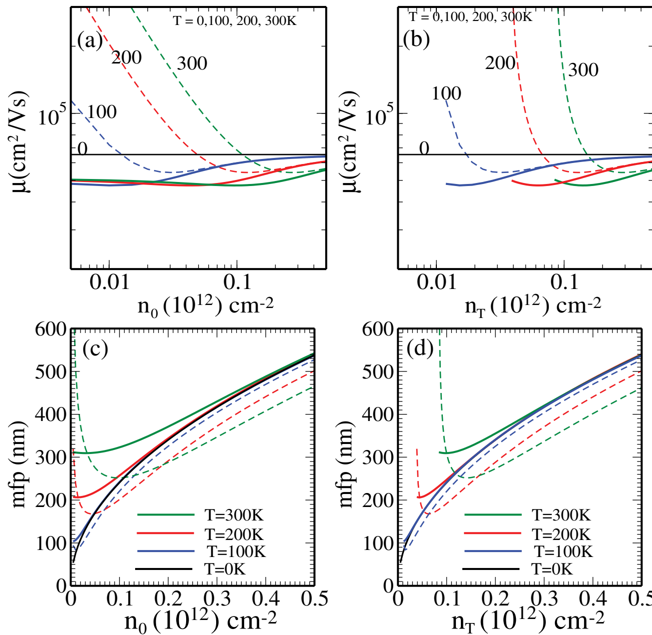

FIG. 7. (Color online) (a), (b) Calculated mobility as a function of density for different temperatures and for a long-range Coulomb potential with $n_i = 10^{10}$ cm^{-2}. Here n_0 indicates the density induced by the gate voltage and $n(T)$ indicates the total density, i.e., the density from the gate plus the density from thermal excitations. Solid lines represent Eq. (40) with $n(T)$ and dashed lines represent Eq. (42) with $n_0 = n(T = 0)$ or density induced by only gate voltage. (c), (d) Mean free path shown as a function of density. Solid (dashed) lines indicate Eq. (41) [Eq. (43)].

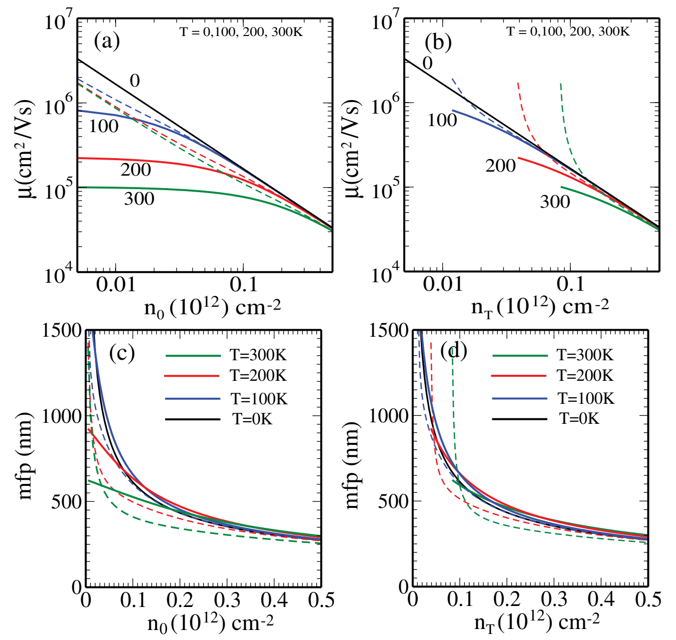

FIG. 8. (Color online) (a), (b) Calculated mobility as a function of density for different temperatures and for a short-range neutral potential with $n_\delta V_\delta^2 = 5$ (eV Å)^2. Solid lines represent Eq. (40) with $n(T)$ and dashed lines represent Eq. (42) with $n_0 = n\ (T = 0)$ or density induced by only the gate voltage. (c), (d) Mean free path shown as a function of density. Solid (dashed) lines indicate Eq. (41) [Eq. (43)].

density $n(T)$ rather than just the doping density n_0, particularly at low carrier densities because the extracted mobility and mean free path for the two definitions differ qualitatively as the Dirac point is approached with the distinction between the two definitions being much larger for long-range disorder. Our work establishes that derived quantities such as mean free path and mobility, which involve an effective division of the experimentally measured conductivity by a density, are not meaningful for graphene (particularly at low densities, approaching the Dirac point) because $n(T)/n_0$ diverges at the Dirac point. This is not a serious problem for graphene on substrates because the puddle-induced cutoff density n_c ensures that $n(T) \approx n_0 \approx n$, but in high-quality SG, mobility and mean free path are meaningful only if they are extracted at a high density where $n(T) \approx n_0$.

All the above results (Figs. 3 and 4) ignore phonon effects, which are very weak in graphene and only affect high-temperature transport. In Figs. 9 and 10, we show the explicit effects of acoustic phonon scattering in the theory by comparing results for $\sigma(T)$ including and excluding phonons in the calculation at high (Fig. 9) and low (Fig. 10) carrier densities and for the Bolotin *et al.*[3,4] and Du *et al.*[1,2] samples. In general, the phonon scattering effect is much stronger for the Bolotin *et al.* sample than the Du *et al.* sample because of the much higher quality (lower disorder) of the former. This finding is completely consistent with our theoretical analysis in Secs. II and III, where we establish that the Dirac point conductivity would be affected by phonons even at rather low temperatures for very clean samples with low values of n_i. Our basic finding is that phonons introduce metallic temperature

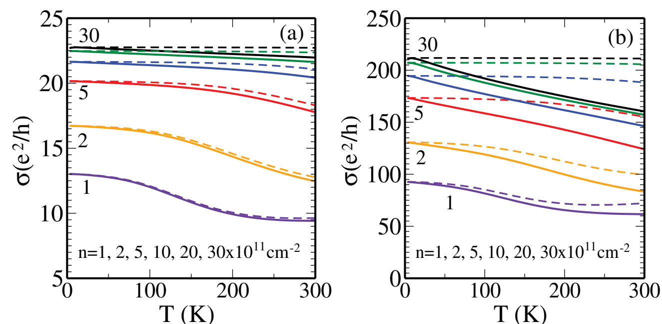

FIG. 9. (Color online) Temperature-dependent conductivity of SG corresponding to the experimental data of (a) Du *et al.*[1] and (b) Bolotin *et al.*[3] The same parameters used in Figs. 3 and 4 are used in this calculation. Solid (dashed) lines indicate the results with (without) phonon scattering.

dependence at higher carrier densities, nullifying the intrinsic insulating temperature dependence arising from Coulomb disorder, but in general the insulating temperature dependence remains quite strong up to the room temperature at a low carrier density (Fig. 10) in high-quality SG. We note that both Figs. 9 and 10 clearly show the very low-temperature ($T/T_F \ll 1$) weak metallic T dependence of $\sigma(T)$ arising entirely from the Fermi surface effect, which is more strongly manifested in the higher-density (Fig. 9) system. This again reinforces our claim that the insulating behavior of $\sigma(n,T)$, which is the hallmark of the Dirac point transport property, is much better studied as a high-temperature phenomenon in low-density SG. This insulating behavior has clearly been observed by Bolotin *et al.*, Du *et al.*, and Mayorov *et al.*, establishing that all three SG samples are reflecting intrinsic Dirac point transport behavior in their very high-quality SG samples. Based on our results we contend that the observation of low-density power-law insulating temperature dependence in graphene is a direct manifestation of the Dirac point behavior.

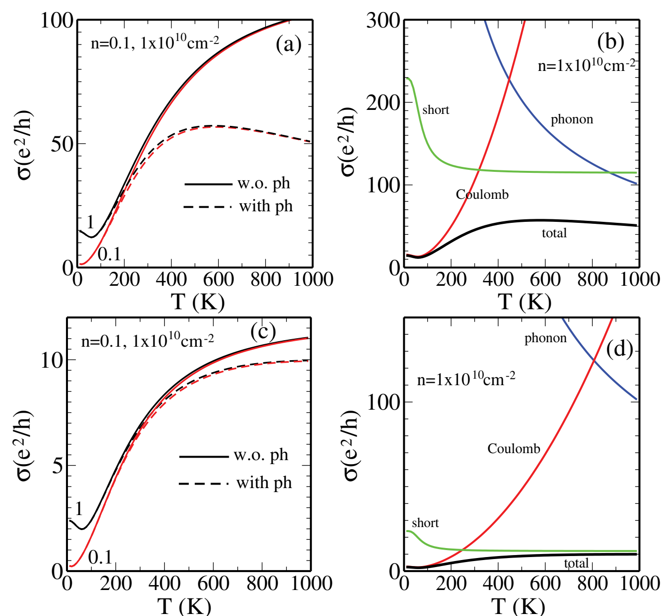

FIG. 10. (Color online) Temperature-dependent conductivity of SG corresponding to the experimental data of (a), (b) Bolotin *et al.*[3] and (c), (d) Du *et al.*[1]. The same parameters used in Figs. 3 and 4 are used in this calculation. (a), (c) Solid (dashed) lines indicate the results without (with) phonon scattering, and black (red) lines indicate the results for a density $n = 10^{10}$ cm^{-2} ($n = 10^{9}$ cm^{-2}). (b), (d) Individual contribution to the total conductivity (black line) is shown for a density $n = 10^{10}$ cm^{-2}. In (d) the nonmonotonic behavior at high densities does not appear due to the strong short-range potential scattering, but in high-mobility samples (b) the nonmonotonic behavior shows up due to the much weaker neutral impurity scatterings.

V. CONCLUSION

We have provided in this work a detailed theoretical study of the density- and temperature-dependent conductivity of low-disorder SG within the semiclassical Drude-Boltzmann transport theory neglecting density inhomogeneity (i.e., puddle) effects. Our theory includes three independent scattering mechanisms: long-range Coulomb disorder, short-range δ-function disorder, and acoustic phonon scattering. We establish, by comparing our detailed numerical results for the conductivity with three recent experimental studies,[1–5] that the measured low-density conductivity in existing experiments on SG is approaching at least some aspects of the intrinsic Dirac point behavior.

Some of our more important qualitative conclusions are as follows. (i) The intrinsic Dirac point behavior is better manifested at higher (lower) temperatures (densities) remaining above the puddle-induced characteristic density. (ii) The observation of a power-law insulating temperature dependence of conductivity is a direct manifestation of the Dirac point behavior. (iii) At low doping densities, it is not meaningful to characterize the system using derived quantities (e.g. mobility or mean free path) because of the considerable ambiguity in which density (just the extrinsic doping density or the total density including thermal excitations) should be used in the definition of mobility (or mean free path). (iv) The competition among long-range and short-range disorder plus phonon scattering could lead to complex (and even nonmonotonic) dependence of the conductivity on temperature and density, and it is not meaningful to conclude about the underlying nature of the transport behavior (ballistic or diffusive; localized or extended, etc.) based just on preconceived notions about the expected density and temperature dependence for various processes. (v) By improving the sample quality and reducing disorder, it should be possible to approach the Dirac point indefinitely through careful conductivity measurements in SG, providing unique opportunities to study in the future many interesting effects not included in our theory (e.g,, interaction, localization, ripple, flexural phonons). (vi) Phonons could affect the Dirac point conductivity in high-quality SG down to arbitrarily low temperatures since the Bloch-Grüneisen temperature becomes vanishingly small near the Dirac point; whether phonon effects will overcome the insulating temperature dependence due to Coulomb disorder depends on the details of the amount of disorder scattering effective in the system.

We conclude by emphasizing that our results establish that how closely in density one has approached the Dirac point can be estimated by seeing how high in temperature the Coulomb-disorder-induced insulating temperature dependence persists in a particular graphene sample (or, paradoxically, how low in

temperature the acoustic phonon effects persist if the graphene sample is devoid of Coulomb disorder causing the insulating behavior).

ACKNOWLEDGMENT

This work was supported by the US ONR.

[1]X. Du, I. Skachko, A. Barker, and E. Y. Andrei, Nat. Nanotechnol. **3**, 491 (2008).

[2]X. Du, I. Skachko, F. Duerr, A. Lucian, and E. Y. Andrei, Nature **462**, 192 (2009).

[3]K. I. Bolotin, K. J. Sikes, Z. Jiang, M. Klima, G. Fudenberg, J. Hone, P. Kim, and H. L. Stormer, Solid State Commun. **146**, 351 (2008); K. I. Bolotin, K. J. Sikes, J. Hone, H. L. Stormer, and P. Kim, Phys. Rev. Lett. **101**, 096802 (2008).

[4]K. I. Bolotin, F. Ghahari, M. D. Shulman, H. L. Stormer, and P. Kim, Nature **462**, 196 (2009).

[5]A. S. Mayorov, D. C. Elias, I. S. Mukhin, S. V. Morozov, L. A. Ponomarenko, K. S. Novoselov, A. K. Geim, and R. V. Gorbachev, Nano Lett. **12**, 4629 (2012).

[6]D. C. Elias, R. V. Gorbachev, A. S. Mayorov, S. V. Morozov, A. A. Zhukov, P. Blake, L. A. Ponomarenko, I. V. Grigorieva, K. S. Novoselov, F. Guinea, and A. K. Geim, Nat. Phys. **7**, 701 (2011).

[7]K. S. Novoselov, A. K. Geim, S. V. Morozov, D. Jiang, Y. Zhang, S. V. Dubonos, I. V. Grigorieva, and A. A. Firsov, Science **306**, 666 (2004).

[8]Y.-W. Tan, Y. Zhang, K. Bolotin, Y. Zhao, S. Adam, E. H. Hwang, S. Das Sarma, H. L. Stormer, and P. Kim, Phys. Rev. Lett. **99**, 246803 (2007).

[9]J. H. Chen, C. Jang, S. Adam, M. S. Fuhrer, E. D. Williams, and M. Ishigami, Nat. Phys. **4**, 377 (2008).

[10]S. Das Sarma, S. Adam, E. H. Hwang, and E. Rossi, Rev. Mod. Phys. **83**, 407 (2011).

[11]S. Das Sarma, E. H. Hwang, and W.-K. Tse, Phys. Rev. B **75**, 121406 (2007).

[12]J. Gonzalez, F. Guinea, and M. A. H. Vozmediano, Nucl. Phys. B **424**, 595 (1994); J. González, F. Guinea, and M. A. H. Vozmediano, Phys. Rev. B **59**, R2474 (1999).

[13]D. V. Khveshchenko, Phys. Rev. Lett. **87**, 246802 (2001); D. T. Son, Phys. Rev. B **75**, 235423 (2007); M. S. Foster and I. L. Aleiner, *ibid.* **77**, 195413 (2008); J. E. Drut and T. A. Lahde, Phys. Rev. Lett. **102**, 026802 (2009); I. F. Herbut, V. Juricic, and B. Roy, Phys. Rev. B **79**, 085116 (2009); J. R. Wang and G. Z. Liu, New J. Phys. **14**, 043036 (2012).

[14]J. Martin, N. Akerman, G. Ulbricht, T. Lohmann, J. H. Smet, K. von Klitzing, and A. Yacoby, Nat. Phys. **4**, 144 (2008).

[15]Y. Zhang, V. Brar, C. Girit, A. Zettl, and M. Crommie, Nat. Phys. **5**, 722 (2009).

[16]J. Xue, J. Sanchez-Yamagishi, D. Bulmash, P. Jacquod, A. Deshpande, K. Watanabe, T. Taniguchi, P. Jarillo-Herrero, and B. J. LeRoy, Nat. Mater. **10**, 282 (2011).

[17]E. H. Hwang, S. Adam, and S. Das Sarma, Phys. Rev. Lett. **98**, 186806 (2007).

[18]S. Adam, E. H. Hwang, V. M. Galitski, and S. Das Sarma, Proc. Natl. Acad. Sci. USA **104**, 18392 (2007).

[19]E. H. Hwang and S. Das Sarma, Phys. Rev. B **77**, 115449 (2008); H. Min, E. H. Hwang, and S. Das Sarma, *ibid.* **83**, 161404 (2011).

[20]K. Kaasbjerg, K. S. Thygesen, and K. W. Jacobsen, Phys. Rev. B **85**, 165440 (2012).

[21]J. H. Chen, C. Jang, S. Xiao, M. Ishigami, and M. S. Fuhrer, Nature Nanotech. **3**, 206 (2008); S. V. Morozov, K. S. Novoselov, M. I. Katsnelson, F. Schedin, D. C. Elias, J. A. Jaszczak, and A. K. Geim, Phys. Rev. Lett. **100**, 016602 (2008).

[22]D. K. Efetov and P. Kim, Phys. Rev. Lett. **105**, 256805 (2010).

[23]T. Ando, A. B. Fowler, and F. Stern, Rev. Mod. Phys. **54**, 437 (1982).

[24]Q. Li, E. H. Hwang, and S. Das Sarma, Phys. Rev. B **84**, 115442 (2011); E. H. Hwang and S. Das Sarma, *ibid.* **82**, 081409 (2010).

[25]E. H. Hwang and S. Das Sarma, Phys. Rev. B **79**, 165404 (2009).

[26]E. H. Hwang and S. Das Sarma, Phys. Rev. B **75**, 205418 (2007).

[27]M. Muller, L. Fritz, and S. Sachdev, Phys. Rev. B **78**, 115406 (2008).

[28]I. L. Aleiner and K. B. Efetov, Phys. Rev. Lett. **97**, 236801 (2006).

[29]X. Wu, X. Li, Z. Song, C. Berger, and W. A. de Heer, Phys. Rev. Lett. **98**, 136801 (2007).

[30]S. V. Morozov, K. S. Novoselov, M. I. Katsnelson, F. Schedin, L. A. Ponomarenko, D. Jiang, and A. K. Geim, Phys. Rev. Lett. **97**, 016801 (2006).

[31]T. Stauber, N. M. R. Peres, and F. Guinea, Phys. Rev. B **76**, 205423 (2007).

[32]A. Ferreira, J. Viana-Gomes, J. Nilsson, E. R. Mucciolo, N. M. R. Peres, and A. H. Castro Neto, Phys. Rev. B **83**, 165402 (2011).

[33]A. Fasolino, J. H. Los, and M. I. Katsnelson, Nat. Mater. **6**, 858 (2007).

[34]E. Mariani and F. von Oppen, Phys. Rev. Lett. **100**, 076801 (2008).

[35]I. V. Gornyi, V. Yu. Kachorovskii, and A. D. Mirlin, Phys. Rev. B **86**, 165413 (2012).

[36]E. Mariani and F. von Oppen, Phys. Rev. B **82**, 195403 (2010).

[37]S. M. Badalyan and F. M. Peeters, Phys. Rev. B **85**, 205453 (2012).

[38]M. Muller, M. Brauninger, and B. Trauzettel, Phys. Rev. Lett. **103**, 196801 (2009).